ORL

Research Article

ORL 2021;83:172–180
DOI: 10.1159/000512731

Received: October 1, 2020
Accepted: October 30, 2020
Published online: February 24, 2021

Relationship between Endolymphatic Hydrops and Symptoms of Meniere Disease in Acoustic Hearing

Yoonkyung Oh[a] Jongwoo Lim[a] Young Sang Cho[b] Namkeun Kim[a]

[a]Department of Mechanical Engineering, Incheon National University, Incheon, Republic of Korea; [b]Department of Otorhinolaryngology-Head and Neck Surgery, Samsung Medical Center, Sungkyunkwan University, School of Medicine, Seoul, Republic of Korea

Keywords
Finite element model · Meniere disease · Basilar membrane · Endolymphatic hydrops · Diplacusis

Abstract
Hypothesis: The endolymphatic hydrops (EH) does not affect hearing loss significantly at low frequencies, whereas the hydrops affects the diplacusis. ***Background:*** There have been many arguments whether the EH cause the Meniere disease. Despite a lot of experimental studies to investigate the Meniere disease, there have been little modeling studies, which are helpful to understand the mechanism. ***Methods:*** A 3D finite element model of the human cochlea and the middle ear was used for investigation of the relationship between EH and hearing loss at low frequencies and diplacusis (2 specific symptoms of Meniere disease). While the cochlear geometry was simplified as a tapered box shape, the middle ear was based on the real geometry obtained from μCT images. EH is implemented by prestress on the basilar membrane surface in the simulation. ***Results:*** The EH did not cause significant hearing loss at low frequencies in both air- and bone-conducted hearing. Rather, this disorder caused a shift in best frequency (BF) position to the base at low frequencies below about 250 Hz. The BF shift can explain the diplacusis because a low-frequency sound can be perceived as a slightly higher frequency so that Meniere patients can perceive 2 different frequency sounds corresponding to a given single-frequency sound. ***Conclusion:*** The EH cannot be a sufficient condition for Meniere disease, whereas the hydrops can cause the diplacusis.

Introduction

Meniere disease (MD) is a disorder of the inner ear first discovered in 1861. The typical symptoms are recurrent vertigo, fluctuating hearing loss accompanying ear fullness, and tinnitus. These are used clinically for the diagnosis of MD. The incidence of MD varies: 157 per 100,000 persons in the UK, 46 per 100,000 in Sweden, 7.5 per 10 0,000 in France [1], and 15 per 100,000 persons in the USA [2]. According to the National Institute on Deafness and Other Communication Disorders, 615,000 individuals in the USA are diagnosed with MD, and 45,500 cases are newly diagnosed each year. MD worsens the quality of life, and research has evaluated how to cope with MD. To date, the exact cause is unknown, but endolymphatic hydrops (EH) is a pathological feature of MD based on enlargement of the endolymphatic volume [3, 4].

karger@karger.com
www.karger.com/orl

Namkeun Kim
Department of Mechanical Engineering
Incheon National University, 119 Academy-ro, Yeonsu-Gu
Incheon 22012 (Republic of Korea)
nkim@inu.ac.kr

Tonndorf used a physical cochlear model to study the effect of EH on fluctuating hearing loss and diplacusis, which are characteristic symptoms of MD [5]. He showed that increased endolymphatic pressure causes (1) a decline in hearing sensitivity, (2) a shift of the location of the maximal amplitude of the basilar membrane (BM) displacement, and (3) harmonic distortion of the BM. Lee and Koike [6] supported this conclusion via a tapered-box finite element (FE) model. They showed a decreased BM velocity (V_{BM}) at low frequency due to prestress applied on the membrane implementing the EH. Merchant et al. [7] reported a different conclusion upon reviewing archival temporal bone cases with MD or EH. They suggested that the EH is a histologic marker for MD rather than being directly responsible for its symptoms. Gürkov et al. [8] supported this different suggestion by analysis of MD patients' high-resolution MR images. They concluded that EH is necessary but not sufficient for a display of the full triad of MD symptoms: vertigo, balance, and hearing disease. Specifically, Cho et al. [9] analyzed the correlation between EH seen in MRI and various audiovestibular tests and showed the various correlation according to each studied case. Although tests other than audiometry were not used in the diagnosis of MD, the EH of cochlea was not sufficient to account for all MD symptoms including hearing loss. In summary, the effects of EH on critical symptoms in MD patients were investigated by physical models, and the conclusion was changed from that EH is a sufficient and necessary condition of MD to a necessary condition.

Here, we show the relationship between EH and characteristic symptoms of MD (i.e., hearing loss at low frequency and diplacusis) using a 3D FE model of the cochlea. The relationship was investigated in air-conducted (AC) hearing as well as bone-conducted (BC) hearing.

It is generally accepted that there are five potential factors for BC stimulation [10]. This study limits the BC factor to the inertial component. In addition, this study does not consider the active amplification mechanism in the BM [11–13]. However, this can be appropriate because the relative V_{BM} would be analyzed corresponding to the existence of prestress on the BM with EH.

Methods

FE Model

We used a 3D FE model with an uncoiled tapered box shape. A detailed geometry and validation of the model was reported previously [14]. A brief description for the model is reported here: The cochlea is composed of scala vestibuli (SV), scala media (SM), and scala tympani (ST). However, SM was combined with SV in the model because it is generally accepted that Reissener's membrane dividing the SV and the SM does not significantly affect the BM motion connected with the auditory nerve [15, 16]. The BM was modeled as an orthotropic material who's Young's modulus in the transverse direction is tenfold higher than that in the longitudinal direction due to the direction of fibers. The fluid in the SV and the ST is connected through the opening on the BM at the apical end, namely, the helicotrema. Figure 1 shows the FE model used here for the human auditory periphery consisting of the middle ear and the cochlea.

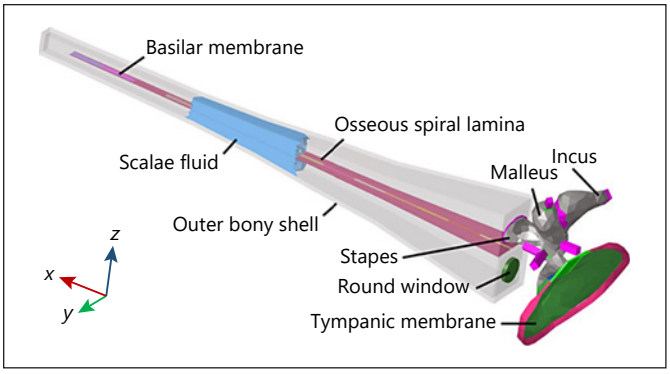

Color version available online

Fig. 1. Posterior-medial view of an FE model of the human auditory periphery consisting of middle ear structure and a simplified uncoiled cochlea. FE, finite element.

The geometries of the middle ear structure, including the TM were obtained by micro-CT [17, 18] and imaging data from human-cadaver temporal bone specimens [19, 20]. The geometry of the cochlear model was based on dimensions published previously [21]. The BM was meshed with 14,000 8-noded hexahedral solid shell elements, and the round window was meshed with 1,700 6-noded pentahedral elements. The 2 fluid chambers, SV and ST, were meshed with 222,000 4-noded linear tetrahedral elements. The material properties used for the current model are summarized in Table 1. The BM mechanical properties are summarized in Table 2.

Air- and Bone-Conduction Stimulation

We assumed that the V_{BM} could quantify the hearing threshold. In other words, a higher V_{BM} implies a lower hearing threshold and vice versa. The V_{BM} was calculated in 2 different stimulation types: AC and BC. AC excitations were simulated by assigning a uniformly dynamic unit pressure over the TM surface on the ear canal side. Fixed displacement boundary conditions were applied to the boundaries of the structure such as the ends of the ligaments and tendons, the edge of the tympanic annulus, the BM support, and the bony shell of the cochlea. Inertial BC excitations were simulated by assigning the same displacement vectors (both magnitude and phase) at the boundaries. These include the cochlea and the ends of the middle-ear supporting structures such as the incus ligament, tensor tympani, anterior ligament, lateral ligament, stapedius tendon, and tympanic annulus. This effectively represented the rigid body vibrations of the temporal bone structure that surrounds the auditory periphery. The rigid body BC excitations were simulated in the z direction (normal to the BM surface; see Fig. 1).

Table 1. Mechanical properties of the model components

Component	Elastic modulus E, Pa	Density ρ, kg/m^3	Loss factor η
Incus	1.41×10^{10}	2.15×10^3	0.01 (constant)
Malleus	1.41×10^{10}	2.39×10^3	0.01 (constant)
Stapes	1.41×10^{10}	2.20×10^3	0.01 (constant)
Incudomalleolar joint	7×10^6	1.20×10^3	0.15 at 1 kHz
Incudostapedial joint	4.4×10^5	1.20×10^3	0.15 at 1 kHz
Tensor tympani	5×10^6	1.20×10^3	0.3 at 1 kHz
Anterior ligament	5×10^6	1.20×10^3	0.3 at 1 kHz
Lateral ligament	10×10^6	1.20×10^3	0.3 at 1 kHz
Superior ligament	2×10^6	1.20×10^3	0.3 at 1 kHz
Stapes tendon	3.8×10^5	1.20×10^3	0.15 at 1 kHz
Incus ligament	4.8×10^6	1.20×10^3	0.15 at 1 kHz
TM, pars tensa	2×10^7	1.20×10^3	0.7 at 1 kHz
TM, pars flaccida	0.7×10^7	1.20×10^3	0.15 at 1 kHz
Tympanic annulus	4×10^5	1.20×10^3	0.3 at 1 kHz
Stapes annular ligament	4.1×10^5	1.20×10^3	0.25 at 1 kHz
Outer bony shell	2.1×10^{15}	5.4×10^3	0.1 (constant)
RW	0.7×10^5	2×10^3	0.857 (constant)
Scalae fluid	1,500, m/s; sound speed	1×10^3	0.1 (constant)

RW, round window.

Table 2. Material properties of the 14 equi-length (2.5 mm) BM sections in the cochlear model

Distance from base, mm	E_{11}, MPa	E_{22}, MPa	E_{33}, MPa	G_{12}, MPa	G_{13}, MPa	G_{23}, MPa	ν_{12}	ν_{13}	ν_{23}
0–2.5	28.240	325.9	28.240	9.9615	9.9615	309.96	0.025995	0.41743	0.3
2.5–5	28.233	315.9	28.233	9.5769	9.5769	299.96	0.026812	0.41708	0.3
5–7.5	28.225	305.9	28.225	9.1923	9.1923	289.96	0.027681	0.41671	0.3
7.5–10	28.217	295.9	28.217	8.8077	8.8077	279.96	0.028608	0.41631	0.3
10–12.5	28.209	285.9	28.209	8.4231	8.4231	269.96	0.029600	0.41589	0.3
12.5–15	28.200	275.9	28.200	8.0385	8.0385	259.96	0.030663	0.41543	0.3
15–17.5	28.190	265.9	28.190	7.6538	7.6538	249.96	0.031805	0.41494	0.3
17.5–20	28.179	255.9	28.179	7.2692	7.2692	239.96	0.033036	0.41441	0.3
20–22.5	28.168	245.9	28.168	6.8846	6.8846	229.96	0.034365	0.41384	0.3
22.5–25	28.156	235.9	28.156	6.5000	6.5000	219.96	0.035806	0.41323	0.3
25–27.5	28.142	225.9	28.142	6.1154	6.1154	209.96	0.037374	0.41255	0.3
27.5–30	28.128	215.9	28.128	5.3708	5.7308	199.96	0.039085	0.41182	0.3
30–32.5	28.112	205.9	28.112	5.3462	5.3462	189.96	0.040959	0.41102	0.3
32.5–35	27.880	122.9	27.880	4.9615	4.9615	106.96	0.068056	0.39940	0.3

Subscripts 1, 2, and 3 mean the *x*, *y*, and *z* directions, respectively, as shown in Fig. 1. BM, basilar membrane.

The FE simulation was performed using the commercial software ACTRAN (MSC software, Newport Beach, CA, USA), which has strength in an analysis of vibro-acoustic problems.

EH Simulation

The calculation was performed in 2 steps to implement the EH in the model. First, a static pressure of 100 Pa was applied to the BM surface to implement the EH. The magnitude of the static pressure was determined based on previous studies showing a pressure difference between endolymph and perilymph [6, 22, 23]. Hereinafter, this deformed BM is called "Meniere 1." However, in "Meniere 1," the magnitude of BM deformation in the height direction (i.e., the z direction in Fig. 1) is larger than the height of the scala fluid chamber. It is impossible for this to occur unless the BM breaks through the cochlear wall. Therefore, we modified the deformed shape of the BM as shown in Fig. 2 considering the co-

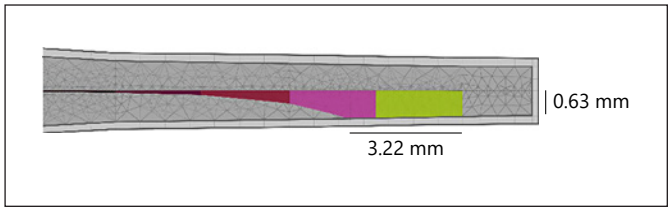

Color version available online

Fig. 2. Side view of the modified BM deformation, "Meniere 2." Colored area represents the deformed BM. BM, basilar membrane.

chlear geometry limitation. Hereafter, this modified model is called "Meniere 2." Next, the dynamic pressure or the sinusoidal displacement was applied to the model (Meniere 1 or Meniere 2) to simulate the AC and BC, respectively.

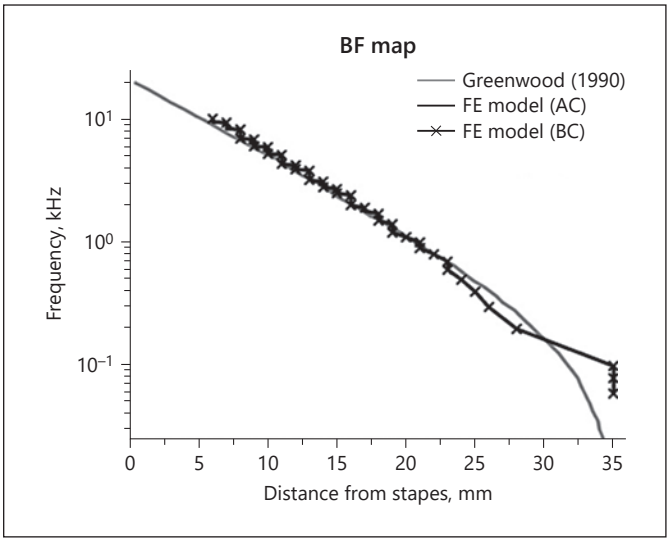

Fig. 3. Comparison of the BF map of the FE model in AC and BC stimulations with experimental data. BF, best frequency; FE, finite element; AC, air-conducted; BC, bone-conducted.

Results

Model Validation

For validation, the best frequency (BF) map of the model was compared to a previous study (Fig. 3). As discussed in the previous study using the same model [14], the BF map was reasonably consistent with that of Greenwood's study [24] regardless of stimulation type, AC and BC. In addition, the V_{BM} 12 mm from the base was also compared with experimental data in both AC and BC [25]. The results showed that simulation responses were reasonably consistent with experimental results. The current study focuses on the V_{BM} differences according to the existence of EH, and V_{BM} in normal conditions are shown in Fig. 4 for validation; a comparison of other responses such as cochlear input impedance and middle-ear transfer function is published [14].

V_{BM} and BF Maps in the Modified Cases

Fig. 5 compares the normalized V_{BM} magnitude of each modified case with the normal case. Meniere 1 and Meniere 2 were compared in the first and second row of Fig. 5, while the AC and BC results are displayed in the first and second columns of Fig. 5, respectively. The normalized factor for AC was the stapes velocity, whereas that for BC was the bone velocity. Each case was calculated in 3 different frequencies: 0.1, 1, and 8 kHz, which represent low, mid, and high frequencies (empty, triangle, and cross, respectively).

Meniere 1 (Fig. 5a, b) shows that when the prestress was applied on the BM surface to implement the EH, the BF position moved about 15 and 7.5 mm to the base at 100 and 1 kHz, respectively, in both AC and BC hearing. There was no change in the BF position at high frequency (8 kHz in AC and BC hearing). The trend of the V_{BM} change at the BF position due to the EH was similar in AC and BC. In both cases, the maximum V_{BM} was nearly the same at low and high frequencies (i.e., 100 and 8 kHz), but it increased about 10 dB due to the EH at mid frequency (1 kHz).

There was 2 different results from Meniere 1 in the case of Meniere 2 (Fig. 5c, d). First, the BF position was moved to the base by about 2.5 mm due to the EH at only the low frequency, 100 Hz, in both AC and BC hearing. Second, the maximum V_{BM} magnitude was decreased by about 5 dB at only the low frequency as well in both AC and BC hearing.

The results of Meniere 1 were based on an unrealistic deformed BM geometry, and it is more reasonable to adopt the Meniere 2 results to represent the effects of EH on hearing loss in the model. However, the observed magnitude of hearing loss in the Meniere 2 cannot be the symptom of MD because ~20 dB of hearing losses at low frequencies is a traditional symptom of MD [26, 27].

Fig. 6 shows the BF maps for normal, Meniere 1, and Meniere 2 cases. In Meniere 1, the prestress could bend the BM enough to change the BF map drastically because the limitation of the ST height was not considered. More specifically, the BF was almost fixed as 12 mm at all the frequencies below about 5 kHz despite the BF position varying corresponding to input frequencies from about 5 to 10 kHz. Meniere 2 showed an almost identical BF map

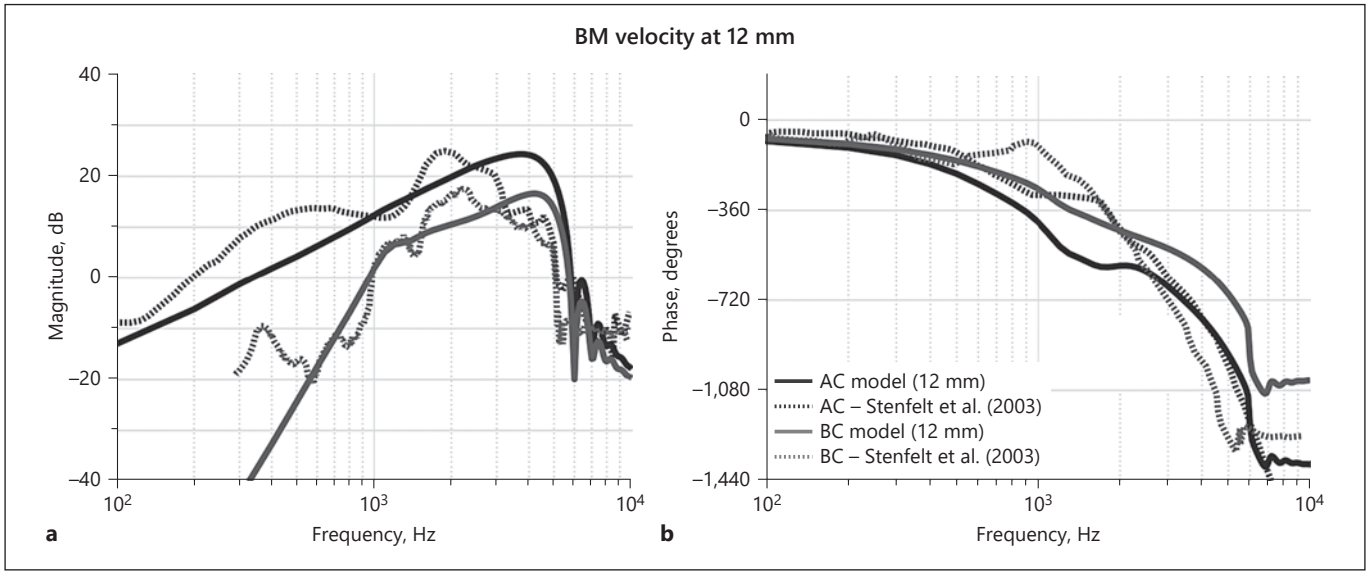

Fig. 4. Comparison of the V_{BM} of the FE model in AC and BC stimulations with experimental data. Magnitude (**a**). Phase (**b**). The velocities were calculated and measured via the model and experiment at 12 mm apart from the base. BM, basilar membrane; FE, finite element; AC, air-conducted; BC, bone-conducted; V_{BM}, BM velocity.

to the normal case except at frequencies below 200 Hz. At low frequencies, the BF position moved maximum 5 mm to the base, which means that a person who has EH may perceive a low-frequency sound as a somewhat higher frequency sound versus a normal person. Similarly, if one has the EH at a single-side ear, then the person can perceive 2 different frequencies corresponding to a given frequency sound. In other words, the sound frequency observed in a normal ear is lower than that in the EH ear and can cause binaural diplacusis.

Discussion

Deformed BM due to the EH

A static pressure of 100 Pa was applied on the BM surface to implement EH in the FE model. As mentioned in the methods, the BM Young's modulus due to the deformed shape was updated for dynamic analysis after applying a static pressure. In contrast, Lee and Koike [6] applied a gradually increasing pressure until 100 Pa on the BM surface resulting in gradual BM deformation. The BM Young's modulus was updated repeatedly. In other words, after the Young's modulus had been calculated the first time due to a slightly deformed shape, an updated Young's modulus was used again in the subsequent calculation of the BM Young's modulus until the BM was no longer deformed due to increasing stiffness. Consequently, the BM Young's modulus in Lee and Koike [6] model is stiffer than that in the current model – this value results in a less deformed BM shape than in our study.

More specifically, Lee and Koike [6] reported that the maximum BM deformation was 60 μm corresponding to a 0 – 100 Pa pressure change over 100 s, which is 1-fold less deformation than that in the current model. According to previous studies, however, the pressure in the endolymph of MD patients is usually beaten periodically rather than applied constantly, and the period is at least 1-fold shorter than 100 s [28]. As a result, the time required to apply pressure on the BM surface is too short to consider repeated calculation for the BM stiffness due to the gradually increased BM deformation. Furthermore, according to previous imaging studies [9, 29], there is significant deformation due to the EH in Reissner's membrane (which is the boarder membrane between SV and SM) rather than BM. Also, according to MRI studies using 3D FLAIR sequences, EH is visualized with sensorineural hearing loss >45 dB, and this supports the hypothesis that EH will develop when medium and high frequencies are involved in MD [30, 31]. Therefore, our results, which is that the deformed BM caused by the EH is not relevant to the low-frequency hearing loss in MD patients, are more comparable to the real patient condition than the previous FE study [6].

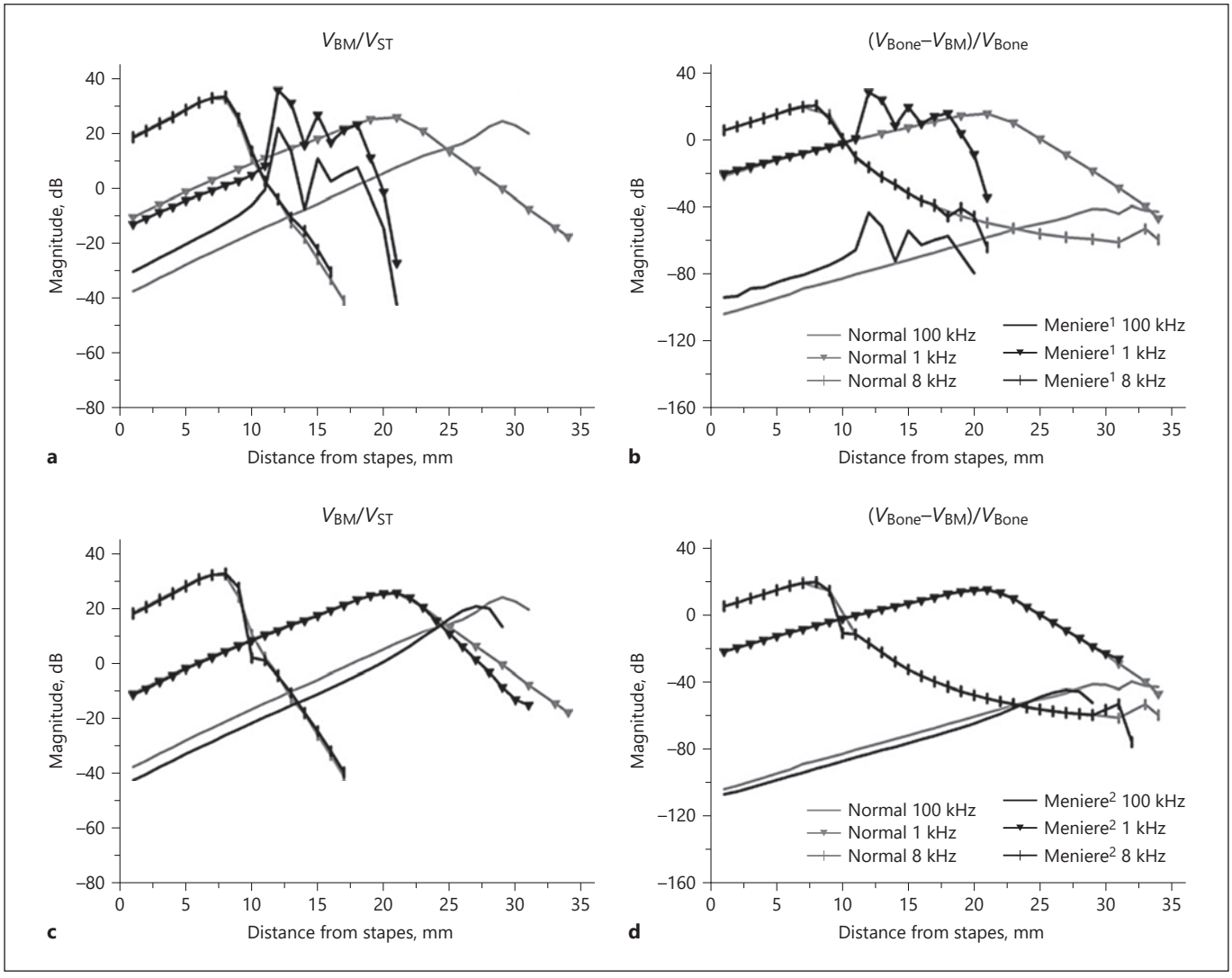

Fig. 5. The normalized V_{BM}. The normalized factors are the stapes velocity and bone velocity in AC and BC, respectively. Each row shows the V_{BM} of each modified case, Meniere 1 (**a, b**) and Meniere 2 (**c, d**). Each column represents V_{BM} in AC and BC stimulations, respectively. While gray lines represent the normal case, black lines describe the modified case. In addition, the triangle and cross marks indicate the V_{BM} at 1 and 8 kHz, respectively. AC, air-conducted; BC, bone-conducted; V_{BM}, BM velocity.

There have been many studies to show the relationship between the EH and hearing loss [32–39]. In these studies, researchers used the MRI to observe the volume change of the endolymphatic fluid space. Therefore, the previous and current studies seem to be contradictory because the premise of the current study is that EH does not cause the low-frequency hearing loss by deforming the BM. However, it should be noted that the current study is focusing on the BM deformation rather than volume changes of endolymphatic fluid space. According to the sequence of pathogenic event leading to MD phenotype, the initial hearing symptoms in MD are tinnitus and low-frequency hearing loss observed during the first attacks of vertigo, and they are not related with the increase of the stiffness of the BM associated with EH [40]. This supports the hypothesis of this study that EH is not an early event in MD.

Diplacusis Caused by EH

Figures 5 and 6 show that the EH shifted the BF position to the basal direction in the current FE simulation. Unfortunately, there have been few clinical studies con-

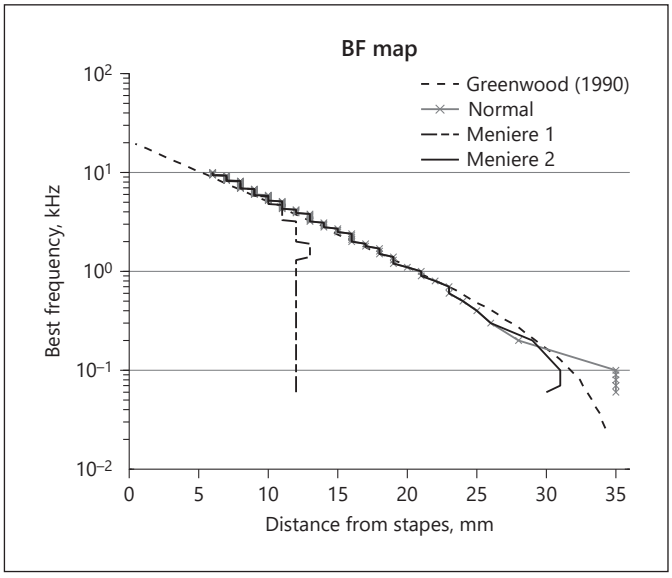

Fig. 6. BF maps of modified cases including the normal case. The results of each case in BC are the same as those in AC cases, respectively. BF, best frequency; AC, air-conducted; BC, bone-conducted.

cerning the frequency change versus any perceived sound in MD patients. Diplacusis is not included in MDs diagnostic criteria, and it has not been properly described or studied in clinical practice. While Ichimiya and Ichimiya [41] recently reported that complex tone stimulation may induce binaural diplacusis when low-tone hearing is impaired, they could not suggest a specific condition or mechanism for the results. The simulation data show that a patient suffering diplacusis can perceive a low-frequency sound as a somewhat higher sound if it is caused by the EH. Furthermore, this misperception should occur at low frequencies below about 250 Hz. Diplacusis may also be caused by a different reason than EH. For instance, Colin et al. [42] showed binaural diplacusis and suggested pitch shift, central neural plasticity, or changes in cochlear mechanics following cochlear damage as the cause of the diplacusis. Therefore, an experiment to indicate the frequency range perceived by a MD patient should be performed to clarify and validate the mechanism of diplacusis. In addition, although not diagnosed with MD, studies to confirm the presence or absence of EH using MRI in normal-hearing patients complaining of diplacusis can also be a clinically interesting topic.

Effects of EH on BC Hearing

The underlying mechanisms for AC and BC are the same as the pressure difference across the BM (antisymmetric pressure component) [14, 43–45]. As expected from the previous studies, there were small differences in cochlear responses between AC and BC because the hydrops implemented by prestress on the BM surface did not affect the fluid pressure across the BM differently to those 2 hearing pathways. This study has limitations in BC analysis because the BC mechanism is simulated by only the inertia of the middle ear and the cochlear fluid [10]. However, it is generally accepted that bone compression becomes a significant factor at high frequencies above 4 kHz, the inertia from the middle ear and cochlear fluid is still the most important factor for BC hearing [46, 47]. Therefore, the current simulation results can be reasonably accepted. In addition, these data suggest that hearing loss at low frequencies in MD patients is sensorineural hearing loss rather than conductive hearing loss.

Clinical Significance and Relevance

In 2015, a committee of the Bárány Society revised the diagnostic criteria such that episodic vertigo and hearing loss accompanied by ear fullness and tinnitus were included in the diagnostic criteria of definite MD [40]. There have been many references to diplacusis or hyperacusis in MD patients, but this is considered a symptom caused by sensorineural hearing loss, but no detailed mechanistic study has been conducted [48]. Recently, with the development of MRI and the image analysis technology, EH can be directly identified by MRI, but the correlation between observed EH and audio-vestibular tests is not always constant. This lack of correlation is likely because the apical middle turn of the cochlea is so small that it is difficult to clearly distinguish the endolymphatic space. In this context, the diagnostic criteria for MD do not require the visualization of EH to confirm the diagnosis of MD as it was stated in the European position statement on diagnosis and treatment of Meniere's disease [49]. Besides, this study proved that low-tone hearing loss in MD is not relevant to the BM deformation due to pressure. In other words, this study suggests that diplacusis may be caused by pressure on the BM even without hearing loss. Therefore, it is necessary to evaluate diplacusis in more detail in patients with suspected MD, which is 1 of the symptoms that is not included in the current diagnostic criteria and has not received significant clinical attention.

Limitation

This study has several limitations. First of all, the present model accounts solely for elevated endolymphatic

space pressure as the only physiologic variable potentially relevant to hydropic symptoms. Therefore, although the model analysis was focused on the low-frequency hearing loss and diplacusis caused by BM deformation, the model is somewhat simplified so it is insufficient to explain other factors such as decoupling of hair cells from the tectorial membrane, major distention of the walls of the membranous labyrinth, cochlear duct, and expansion of the volume of the endolymphatic space. Furthermore, there may be compartmentalization of these pathologic factors that may not be uniform throughout all segments of the cochlea. This also needs to be considered. However, based on the real geometry, the BM geometry of the model was varied along the length in width and thickness, and the cross-sectional area of the cochlear fluid chamber was also varied along the length. In addition, the BM responses with this consideration of the real geometry were validated in several previous studies [14, 50–52]. Therefore, the results of this study relevant to BM deformation can be meaningful to understand the MD.

Conclusion

Two different symptoms of MD – hearing loss at low frequencies and diplacusis – were investigated by a 3D FE model of human cochlea and validated by comparison with previous studies. The results of this study can conclude that (1) the increased stiffness of the BM associated with EH may explain diplacusis in patients with MD, and (2) hearing loss at low frequencies is not associated with the increased stiffness of the BM associated with EH.

Acknowledgements

The authors thank Prof. S.H.Hong, Prof. W.H.Chung, and Prof. I. Moon at Samsung Medical Center for their precious comments.

Statement of Ethics

The approval from the Ethic Committee was not needed because the results were not obtained from any human or animal subjects but from model simulation.

Conflict of Interest Statement

The authors declare that they have no conflict of interest to disclose.

Funding Sources

This work was supported by the Incheon National University Research Grant in 2017.

Author Contributions

Conceptualization: Y.S. Cho and N. Kim; validation: J. Lim; formal analysis and investigation: Y. Oh.; writing – original draft preparation: Y. Oh; writing – review and editing: Y.S. Cho and N. Kim; supervision: N. Kim. All authors have read and agreed to the published version of the manuscript.

References

1 Reeves DL, Stuck RM. Clinical and experimental results with thorotrast. Medicine. 1938;17(1):37–74.
2 Wladislavosky-Waserman P, Facer GW, Mokri B, Kurland LT. Meniere's disease: a 30-year epidemiologic and clinical study in rochester, MN, 19—1980. Laryngoscope. 1984; 94(8):1098–102.
3 Hallpike CS, Cairns H. Observations on the pathology of Ménière's syndrome: (section of otology). Proc R Soc Med. 1938 Sep;31(11): 1317–36.
4 Klis JF, Smoorenburg GF. Cochlear potentials and their modulation by low-frequency sound in early endolymphatic hydrops. Hear Res. 1988;32(2–3):175–84.
5 Tonndorf J. The mechanism of hearing loss in early cases of endolymphatic hydrops. Ann Otol Rhinol Laryngol. 1957;66(3):766–84.
6 Lee S, Koike T. Simulation of the basilar membrane vibration of endolymphatic hydrops. Procedia IUTAM. 2017;24:64–71.
7 Merchant SN, Adams JC, Nadol JB. Pathophysiology of Ménière's syndrome: are symptoms caused by endolymphatic hydrops? Otol Neurotol. 2005;26(1):74–81.
8 Gürkov R, Pyykö I, Zou J, Kentala E. What is Menière's disease? a contemporary re-evaluation of endolymphatic hydrops. J. Neurol. 2016;263(1):71–81.
9 Cho YS, Ahn JM, Choi JE, Park HW, Kim YK, Kim HJ, et al. Usefulness of intravenous Gadolinium inner ear MR imaging in diagnosis of Ménière's disease. Sci Rep. 2018 Dec;8(1): 17562.
10 Stenfelt S, Goode RL. Bone-conducted sound: physiological and clinical aspects. Otol Neurotol. 2005 Nov;266:1245–61.
11 Ren T. The cochlear amplifier and Ca2+ current-driven active stereocilia motion. Nat Neurosci. 2005 Feb;8(2):132–4.
12 Shera CA. Laser amplification with a twist: traveling-wave propagation and gain functions from throughout the cochlea. J Acoust Soc Am. 2007 Nov;122(5):2738.
13 Spector AA, Ameen M, Schmiedt RA. Modeling 3-D deformation of outer hair cells and their production of the active force in the cochlea. Biomech Model Mechanobiol. 2002; 1(2):123–35.
14 Kim N, Homma K, Puria S. Inertial bone conduction: symmetric and anti-symmetric components. J Assoc Res Otolaryngol. 2011;12(3): 261–79.
15 Steele CR. Behavior of the basilar membrane with pure-tone excitation. J Acoust Soc Am. 1987 Jan;55(1):148–62.

16 Chan WX, Yoon YJ, Kim N. Mechanism of bone-conducted hearing: mathematical approach. Biomech Model Mechanobiol. 2018; 17(6):1731–40.
17 Homma K, Du Y, Shimizu Y, Puria S. Ossicular resonance modes of the human middle ear for bone and air conduction. J Acoust Soc Am. 2009 Feb;125(2):968–79.
18 Homma K, Shimizu Y, Kim N, Du Y, Puria S. Effects of ear-canal pressurization on middle-ear bone- and air-conduction responses. Hear Res. 2010;263(1–2):204–15.
19 Sim JH, Puria S. Soft tissue morphometry of the malleus-incus complex from micro-CT imaging. J Assoc Res Otolaryngol. 2008 Mar; 9(1):5–21.
20 Sim JH, Puria S, Steele C. Calculation of inertial properties of the malleus-incus complex from micro-CT imaging. J Mech Mater Struct. 2007;2(8):1515–24.
21 Thorne M, Salt AN, DeMott JE, Henson MM, Henson OW, Gewalt SL. Cochlear fluid space dimensions for six species derived from reconstructions of three-dimensional magnetic resonance images. Laryngoscope. 1999 Oct; 109(10):1661–8.
22 Böhmer A, Andrews JC. Maintenance of hydrostatic pressure gradients in the membranous labyrinth. Arch Otorhinolaryngol. 1989; 246(1):65–6.
23 Ito S, Fisch U, Dillier N, Pollak A. Endolymphatic pressure in experimental hydrops. Arch Otolaryngol Head Neck Surg. 1987; 113(8):833–5.
24 Greenwood DD. A cochlear frequency-position function for several species–29 years later. J Acoust Soc Am. 1990 Jun;87(6):2592–605.
25 Stenfelt S, Puria S, Hato N, Goode RL. Basilar membrane and osseous spiral lamina motion in human cadavers with air and bone conduction stimuli. Hear Res. 2003 Jul;181(1–2): 131–43.
26 Muchnik C, Hildesheimer M, Rubinstein M, Arenberg IK. Low frequency air-bone gap in Meniere's disease without middle ear pathology. a preliminary report. Am J Otol. 1989 Jan;10(1):1–4.
27 Yetiser S, Kertmen M. Cochlear conductive hearing loss in patients with Meniere's disease. Kulak Burun Bogaz Ihtis Derg. 2007; 17(1):18–21.
28 Valk WL, Wit HP, Albers FWJ. Rupture of Reissner's membrane during acute endolymphatic hydrops in the guinea pig: A model for Ménière's disease? Acta Otolaryngol. 2006 Oct;126(10):1030–5.
29 Fraysse BG, Alonso A, House WF. Menière's disease and endolymphatic hydrops: clinical-histopathological correlations. Ann Otol Rhinol Laryngol Suppl. 1980 Nov;89(6 Pt 3):2–22.
30 Attyé A, Michael E, Maud M, Irène T, Georges D, Alexandre K, et al. In vivo imaging of saccular hydrops in humans reflects sensorineural hearing loss rather than Meniere's disease symptoms. Eur Radiol. 2018 Jul;28(7): 2916–22.
31 Lopez-Escamez JA, Attyé A. Systematic review of magnetic resonance imaging for diagnosis of Meniere disease. J. Vestib. Res. 2019; 29(2–3):121–9.
32 Gürkov R, Flatz W, Louza J, Strupp M, Krause E. In vivo visualization of endolyphatic hydrops in patients with Meniere's disease: correlation with audiovestibular function. Eur Arch Otorhinolaryngol. 2011 Dec;268(12): 1743–8.
33 Seo YJ, Kim J, Choi JY, Lee WS. Visualization of endolymphatic hydrops and correlation with audio-vestibular functional testing in patients with definite Meniere's disease. Auris Nasus Larynx. 2013 Apr;40(2):167–72.
34 Wu Q, Dai C, Zhao M, Sha Y. The correlation between symptoms of definite Meniere's disease and endolymphatic hydrops visualized by magnetic resonance imaging. Laryngoscope. 2016 Apr;126(4):974–9.
35 Jerin C, Floerke S, Maxwell R, Gürkov R. Relationship between the extent of endolymphatic hydrops and the severity and fluctuation of audiovestibular symptoms in patients with menière's disease and mri evidence of hydrops. Otol Neurotol. 2018 Feb;39(2): e123–e130.
36 Shi S, Guo P, Li W, Wang W. Clinical features and endolymphatic hydrops in patients With MRI evidence of hydrops. Ann Otol Rhinol Laryngol. 2019 Apr;128(4):286–92.
37 Gürkov R, Berman A, Dietrich O, Flatz W, Jerin C, Krause E, et al. MR volumetric assessment of endolymphatic hydrops. Eur Radiol. 2015 Feb;25(2):585–95.
38 Fiorino F., Pizzini FB, Beltramello A, Barbieri F. Progression of endolymphatic hydrops in Ménière's disease as evaluated by magnetic resonance imaging. Otol Neurotol. 2011 Sep; 32(7):1152–7,
39 Jerin C, Krause E, Ertl-Wagner B, Gürkov R. Longitudinal assessment of endolymphatic hydrops with contrast-enhanced magnetic resonance imaging of the labyrinth. Otol Neurotol. 2014;35(5):880.
40 Lopez-Escamez JA, Carey J, Chung W H, Goebel J A, Magnusson M, Mandalà M, et al. Diagnostic criteria for Meniere's disease. J Vestib Res. 2015;25(1):1–7.
41 Ichimiya I, Ichimiya H. Complex tone stimulation may induce binaural diplacusis with low-tone hearing loss. PLoS One. 2019;14(1): e0210939.
42 Colin D, Micheyl C, Girod A, Truy E, Gallégo S. Binaural diplacusis and its relationship with hearing-threshold asymmetry. PLoS One. 2016;11(8):e0159975.
43 Békésy Gv. Zur theorie des hörens bei der schallaufnahme durch knochenleitung. Ann. Phys. 1932 Jan;405(1):111–36.
44 Stenfelt S. Simultaneous cancellation of air and bone conduction tones at two frequencies: extension of the famous experiment by von Bekesy. Hear. Res. 2007 Mar;225(1–2): 105–16.
45 Tasaki I, Davis H, Legouix J -P. The space-time pattern of the cochlear microphonics (guinea pig), as recorded by differential electrodes. J Acoust Soc Am. 1952 Sep;24(5):502–9.
46 Stenfelt S. Inner ear contribution to bone conduction hearing in the human. Hear Res. 2015;329:41–.
47 Stenfelt S. Model predictions for bone conduction perception in the human. Hear Res. 2016 Oct;340:135–43.
48 Parker W. Meniere's disease: etiologic considerations. Arch Otolaryngol Head Neck Surg. 1995;121(4):377–82.
49 Magnan J, Nuri Özgirgin O, Trabalzin F, Lacour M, Lopez Escamez A, Magnusson M, et al. European position statement on diagnosis, and treatment of Meniere's disease. J Int Adv Otol. Aug 2018;14(2):317–21.
50 Kim N, Steele CR, Puria S. Superior-semicircular-canal dehiscence: effects of location, shape, and size on sound conduction. Hear. Res. 2013;301:72–84.
51 Kim N, Steele CR, Puria S. The importance of the hook region of the cochlea for bone-conduction hearing. Biophys J. 2014;107(1):233–41.
52 Lim J, Kim Y, Kim N. Mechanical effects of cochlear implants on residual hearing loss: a finite element analysis. IEEE Trans Biomed Eng. 2020 Mar;67(11):3253–61.